This is a repository copy of *Longitudinal effects of Parathyroid Hormone treatment on morphological, densitometric and mechanical properties of mouse tibia*.

White Rose Research Online URL for this paper:
https://eprints.whiterose.ac.uk/119571/

Version: Accepted Version

ORIGINAL PAPER:

Longitudinal effects of Parathyroid Hormone treatment on morphological, densitometric and mechanical properties of mouse tibia.

Yongtao Lu, PhD[1,2, 3,#], Maya Boudiffa, PhD[4#], Enrico Dall'Ara, PhD[3,4], Yue Liu[1], Ilaria Bellantuono, MD, PhD[3,4], Marco Viceconti, PhD[2,3]

[1]Department of Engineering Mechanics, Dalian University of Technology, Dalian, China

[2]Department of Mechanical Engineering, the University of Sheffield, Sheffield, UK

[3]Insigneo Institute for in silico Medicine, the University of Sheffield, Sheffield, UK

[4]MRC Arthritis Research UK Centre for Integrated research into Musculoskeletal Ageing (CIMA), Department of Oncology and Metabolism, the University of Sheffield, Sheffield, UK

[#]These authors contributed equally to this work.

CORRESPONDING AUTHOR:

Enrico Dall'Ara, PhD

Department of Oncology and Metabolism and INSIGNEO Institute for in silico Medicine,

University of Sheffield, Sheffield, UK

Phone: +44 (0)114 2226175

Email: e.dallara@sheffield.ac.uk

ABSTRACT:

The use of Parathyroid Hormone (PTH) as bone anabolic is limited due to cost-benefit assessments. Preclinical studies evaluating the effects of PTH on bone have reported variable and often contradictory results. Here, we have applied a new approach using a combination of *in-vivo* longitudinal μCT, image processing techniques and finite element models to monitor early local changes in the whole tibia (divided in 40 compartments) and mechanical properties of female C57BL/6J mice treated with PTH 1-34, compared to controls. Compared with standard 3D bone morphometric analysis, our new approach allowed detection of much smaller and localised changes in bone mineral content (BMC) at very early time points (1 week vs 3 weeks with standard methods) and showed that changes do not occur uniformly over time and across the anatomical space. Indeed, in the PTH treated mice, significant changes in BMC were observed in the medial and posterior sectors of the proximal tibia, a week after treatment, and in the medial sector of the tibia midshaft region a week later ($p < 0.05$). By the third week, two thirds of the regions showed significantly higher values of BMC ($p < 0.05$). The effect of PTH on bone regional volume is similar to that on BMC, but there is almost no effect of PTH on bone tissue mineral density. The differences in estimated mechanical properties became significant after three weeks of treatment ($p < 0.05$). These results provide the first evidence of an early and localised PTH effect on murine bone, and show that our novel partitioning approach, compared to the standard evaluation protocol, allows a more precise quantification of bone changes following treatment, which would facilitate preclinical testing of novel mono- and/or combination therapies throughout the bone.

KEY WORDS: PTH, bone remodeling, animal models, micro-CT, bone quantification.

1 Introduction

Osteoporotic fractures are a major clinical problem that increases the mortality and morbidity of our ageing society [1, 2]. Despite being the only FDA approved anabolic drug for the treatment of osteoporosis [3], teriparatide (PTH 1-34) is recommended for use only as secondary line of intervention due to cost-benefit considerations. Therefore, finding ways to reduce teriparatide dosage while still retaining its positive effects is the focus of intense investigation [4].

Preclinical studies are useful tools to understand how this may be achieved. However, testing for the effect of parathyroid hormone (PTH) on bone in mono- or combination therapy has reported variable results in mice [5-8]. This is thought to be due to the cross-sectional design of the studies, which limits the power to detect meaningful differences, and to the way the 3D bone micro-architecture is analysed, by using sample regions (e.g. the proximal/distal region and/or the midshaft region of long bones), thus underrepresenting the response of the whole bone [9-11]. PTH has been shown to increase trabecular bone density and femoral strength measured by three-points bending mechanical testing in juvenile [12], young [13] and adult [14] mice. This *ex vivo* approach allows only for comparison of mechanical properties between groups of different animals in standard cross-sectional designs, including the intrinsic inter-subject variability and limiting the power of detecting small longitudinal changes in the same animals. Furthermore, three-points bending tests are affected by experimental artefacts [15] and are scarcely informative of the changes in bone strength due to changes in the cortical and trabecular bone properties in different regions of the bone.

In vivo imaging techniques can be used to non-invasively analyse the same tissues of the same mice longitudinally, reducing the measurement variability due to inter-subject differences [16]. In particular, the combination of *in vivo* micro computed tomography (μCT) and image registration improve the measurement of bone properties by reducing

measurements uncertainties [17]. Recently this approach has been used to study in mice models the effect of interventions and/or mechanical loading on bone remodelling in the trabecular centrum of the caudal vertebrae [18-20], in the proximal tibia [21-23] or in the tibia midshaft [24, 25]. However, little is known about early spatiotemporal effects of PTH on the morphological and densitometric properties of the whole mice bones. The three-dimensional μCT images of the mouse tibia can be converted into finite element (FE) models for non-invasive estimation of its mechanical properties [26, 27]. *In vivo* μCT-based FE models of bone portions have been used to investigate the relationship between bone remodeling and mechanical stimuli in para-physiological loading conditions [19, 28] and to study bone healing [29]. To the authors' knowledge no studies have used the *in vivo* μCT-based FE models to reveal longitudinal changes in the whole tibia mechanical properties and their relations with the spatiotemporal changes of bone morphological and densitometric properties. This would be fundamental to understand if the pre-clinically tested intervention would be effective in improving the bone competence of resisting fractures, which is the final clinical goal of anti-osteoporosis treatments.

The aim of this study is to quantify longitudinal effects of PTH on the properties on the tibia of female C57BL/6J mice by using a combination of *in vivo* μCT imaging, image processing and finite element analysis.

2 Material and Methods:

2.1 Animals and treatment

Ten 13-weeks-old female C57BL/6J mice were purchased from Harlan Laboratories (Bicester, UK). They were housed in the University of Sheffield's Biological Services Unit with a twelve-hour light/dark cycle at 22°C and free access to food and water. All the procedures complied with the UK Animals (Scientific Procedures) Act 1986 and were

reviewed and approved by the local Research Ethics Committee of the University of Sheffield (Sheffield, UK). At 18 weeks of age, mice (n=5/group) received a daily i.p. injection of either PTH (hPTH 1-34, Bachem, Bubendorf, Switzerland) at 100 ng/g/day 7 days a week ("WT+PTH" group) or vehicle ("WT" group). PTH was prepared in 1% acetic acid and 2% heat inactivated mouse serum in HBSS (Hank's Balanced Salt Solution, Gibco®). The treatment was given until the age of 22 weeks (end of the experiment).

2.2 In-vivo µCT imaging

The whole right tibia of the mice was imaged using the Scanco *in-vivo* µCT (vivaCT 80, Scanco Medical, Bruettisellen, Switzerland). A baseline scan was performed at 14 weeks of age, then weekly follow up scans starting the second week after the initial scan, for seven weeks (Figure 1). The scanner was operated at 55 keV, 145 µA, 32 mm FOV, 1500/750 samples/projections, 200ms integration time and a nominal isotropic image voxel size of 10.4 µm. A third-order polynomial beam hardening correction algorithm provided by the manufacturer, determined using the 1200 mg HA/cm^3 wedge phantom, was applied to all the scans. The image grey values were then converted into HA-equivalent BMD values by means of the calibration law suggested by the manufacturer and based on weekly quality check performed with a five-rod densitometric calibration phantom.

As *in vivo* µCT imaging is based on ionising radiation, there is an effect on the biological response of the imaged animal, which may affect the outcomes of the study. Taking into account this effect, we used the same scanning procedure for both groups at each time step and we reported data normalized for the baseline scans. The chosen scanning protocol induced 513 mGy dose to the mouse. Previous studies on C57BL/6J mice reported that repeated scans inducing 776 mGy affect significantly only trabecular bone and scans inducing 434 mGy were found not to affect cortical nor trabecular parameters [30].

Therefore, in order to evaluate the radiation effect with our scanning protocol, at the end of the longitudinal study we compared the bone mineral content in the scanned and the non-irradiated contra-lateral tibiae.

2.3 Standard 3D morphometric analysis

For trabecular bone analysis, a region of 1.0 mm height was chosen 0.2 mm below the growth plate as previously described [31].For cortical bone analysis, a region of 1.0 mm height was chosen in the tibia midshaft [31]. Regions of interest for each compartment were manually marked and 3D bone parameters were generated, namely: trabecular bone volume fraction (BV/TV), number (Tb.N), separation (Tb.Sp) and thickness (Tb.Th) and average cortical thickness (Ct.Th).The analyses were performed with the software provided by the manufacturer of the μCT (V6.5-3, Scanco Medical, Bruettisellen, Switzerland).

2.4 Image processing and 4D analyses analysis

Image processing was performed as previously described [31]. Briefly, rigid registration was applied to align tibiae along the longitudinal axis and to achieve correct rotation around this axis. For the registration, the tibia from the baseline scan was taken as the reference [27]. The tibiae from the following scans and from other mice were rigidly registered to the tibia of the baseline using a Quasi-Newton optimizer and the Euclidean distance as the similarity measure (Amira 5.4.3, FEI Visualization Sciences Group, France). Afterwards, the tibiae were divided in different regions and the bone properties in each region were tracked in time. In particular, after the image transformation, the tibial length (L) was measured from tibial most proximal voxel to the most distal voxel and a region of 80% of L was cropped out starting from the area below the proximal growth plate (Matlab, 2015a, The Mathworks, Inc. USA). Then, the obtained volume of interest (VOI) was partitioned into compartments

(Figure 2) using an in-house developed Matlab code. In the tibial longitudinal (proximal-distal) direction, the VOI was divided into ten regions with the same length to minimise the effect of tibial growth on the measured data. Each tibial transverse (x-y) section was then divided into four sectors (anterior, medial, posterior and lateral sectors) by two straight crossing lines passing through the centre of mass of each slice (Figure 2). This step was implemented in order to account for the small (but still significant) growth of the tibia after week 14 which would affect dramatically the measurement of bone changes if a method based on rigid registration and Boolean operation would be used [31, 32]. Our approach implicitly assumes that after week 14 the growth can be considered affine, with homogeneous growth along the longitudinal direction. The greyscale VOI datasets were smoothed with a Gaussian filter (convolution kernel [3 3 3], standard deviation = 0.65) and then binarised using 25.5% of the maximal greyscale value in order to isolate bone voxels [33] and to reduce the effect of the image noise. The bone mask was then obtained from the binarised images. The bone mineral content (BMC) and bone volume (BV) were calculated as the sum of bone mineral (obtained from the greyscale images) and bone volume over the total and regional masked bone regions. The regional bone tissue mineral density (TMD) was calculated as the mean mineral density within the masked bone regions.

Changes of tibial bone parameters (BP), including BMC, BV and TMD in each compartment were represented as the mean relative percentage difference between the intervention (WT+PTH) and the control (WT) groups. First, for each week (*j*), in each compartment, the mean changes in BP relative to the baseline values for the control (ΔA_j) and PTH treated (ΔB_j) groups were calculated as below:

$$\Delta A_j = \frac{\sum_{i=1}^{n1}\left(BP1_{i,j} - BP1_{i,14}\right)}{n1} \tag{1}$$

$$\Delta B_j = \frac{\sum_{i=1}^{n2}\left(BP2_{i,j} - BP2_{i,14}\right)}{n2} \tag{2}$$

where, $n1$ and $n2$ are the numbers of mice in control (BP1) and PTH (BP2) groups; j represents the week index and i represents the mouse number index.

Then for each week, in each compartment, the difference between the control (ΔA_j) and PTH treated groups (ΔB_j) normalized to the average BP of the control at that week, which is defined as the mean relative percentage difference ($\delta D\%_j$), was calculated as below.

$$\delta D\%_j = \frac{(\Delta B_j - \Delta A_j)}{REF_j} \times 100 \tag{3}$$

where,

$$REF_j = \frac{\sum_{i=1}^{n1} BP1_{i,j}}{n1}$$

The precision error for this procedure was found to be less than 3.0% [31], therefore, only changes in BMC and BV lower than -3.0% or greater than +3.0% will be considered for interpretation.

2.5 Finite element models

Subject-specific micro-FE (µFE) models of each tibia at each time point were generated. A connectivity filter was used to clean the binarized VOI image datasets from all unconnected bone islands (by keeping a face-to-face connectivity). The resulting dataset was directly converted into 8-node hexahedral element mesh using a well-established procedure recently validated for trabecular bone samples [34]. Bone was modelled as homogenous, isotropic, and linear elastic, with a module of elasticity of 14.8 GPa, and Poisson's ratio of 0.3 [35, 36]. The tibia compressive stiffness and failure load were calculated by fully constraining the proximal part of the VOI and by applying a displacement of 0.05mm along the tibial longitudinal axis to the distal side of the VOI. The tibiae were aligned using the image rigid registration, which assured that the tibiae were tested in the same loading

8

condition among animals and time points. The compressive stiffness was computed as the total reaction forces divided by the applied displacement.

The resulting linear μFE models were solved (Ansys, Release 14.0.3, ANSYS, Inc.) on a workstation (Intel Xeon E-5-2670. 2.60 GHz, 256 GB RAM) in approximately 75 minutes.

2.6 Statistical analysis

The standard 3D morphological parameters (BV/TV, Tb.N, Tb.Sp, Tb.Th and Ct.Th), the regional BMC, BV and TMD, total BMC, FE predicted stiffness and failure load were analysed using the Analysis of Covariance (ANCOVA) (adjust for the baseline values at week 14) to test the effect of PTH intervention. Analysis was performed in R software (https://www.r-project.org/). Data are presented as mean ± standard deviation (SD) unless otherwise specified, and p values <0.05 are considered statistically significant. Linear regression equations and the coefficients of determination (R^2) were computed for relationships between tibial BMC and stiffness calculated with the FE models.

3 Results

3.1. Effect of irradiation on BMC

The total BMC measured at week 22 culling the animals on the non-irradiated tibia was lower than that measured on the irradiated tibia. Similar differences between non-irradiated and irradiated tibiae were found for both PTH intervention (WT+PTH) and control (WT) groups (5.8±1.9%, range 3.7-8.0% for control group; 5.1±0.9%, range 3.9-6.1% for PTH intervention group). Therefore, considering that similar differences were found for both intervention and vehicle groups we believe that our approach is reliable for evaluating the changes induced by PTH.

3.2. Effect of PTH treatment on bone morphometric and densitometric properties

The standard 3D analysis revealed a significantly higher midshaft Ct.Th (p<0.0001) in response to PTH three weeks after treatment. Trabecular BV/TV, Tb.Th and Tb.N did not significantly change following PTH treatment (Table1).

The spatiotemporal analysis showed significant effects of treatment on BMC changes with respect to baseline, already after one week, localised in the most proximal sub volumes of the tibia (C01: + 7% *vs* WT; p<0.05 for posterior sector and + 9% *vs* WT; p<0.05 for medial sector). After two weeks of treatment, this effect is extended to other regions of the metaphysis and towards the diaphysis (anterior sectors: +11%, p<0.01 for C01; +8%, p<0.05 for C02; posterior sectors: +9%, p<0.05 for C01 and +10%, p<0.01 for C02; medial sectors: +9%, p<0.05 for C01; +11%, p<0.05 for C04; +9%, p<0.05 for C05). By the 3rd week of treatment, most of the sectors (34 out of 40) showed significant anabolic effect of PTH (ranging from +7% to +24%; p<0.05); which reached all sectors but two (in the distal portion of the lateral compartment, p>0.05) by the end of the experiment (Figure 3). The 95% confidence intervals are reported in the supporting material (Supplemental Table S1 and Supplemental Table S2). The spatiotemporal analysis also showed the effect of PTH on tibial regional BV is very similar to that on BMC (Supplemental Figure S1) and there is no effect of PTH on tibial regional TMD (Figure 4).

3.4. Tibial stiffness, total BMC and their correlations

In both control and PTH intervention groups, the normalized total BMC and the normalized FE predicted stiffness increased from baseline values. The increase of both properties in the PTH intervention group after three weeks (week 21) of treatment were higher than those measured for the control group. The values normalized with respect to the baseline of the PTH intervention and control groups were 42.3±5.7% vs 25.9±6.7% for total

BMC and 24.3±5.4% vs 14.1±1.9% for FE predicted stiffness (both p<0.05, Figure 5). Larger differences between control and PTH intervention groups were found after four weeks (week 22) of treatment (48.7±6.2% vs 27.9±5.9% for total BMC and 30.4±6.4% vs 13.4±3.3% for FE predicted stiffness, respectively; both p<0.01, Figure 5).

The FE predicted tibial stiffness was highly linearly correlated with tibial total BMC for both pooled data (R^2 equal to 0.88) and data separated between PTH intervention (R^2 equal to 0.92) and vehicle (R^2 equal to 0.81) groups (Figure 6).

4 Discussion

In this study, we have investigated the longitudinal effects of PTH on the morphometric (BT/TV, Tb.N, Tb.Sp, Tb.Th, Ct.Th and BV), densitometric (BMC and TMD) and mechanical properties (stiffness and failure load) of the tibia of female C57BL/6J mice.

Our data revealed early localised BMC changes following PTH treatment, which could not be detected using the standard morphometric analysis restricted to small trabecular and cortical regions of interest. This is probably due to the more comprehensive and detailed spatiotemporal measurements (performed with our approach) over the whole tibia, the information of which can hardly be provided by the standard morphometric analysis. Indeed, this anabolic statistically significant effect started in the most proximal region of the tibia at the posterior and medial sectors, progressively spreading in the proximal-distal direction and becoming significant in most compartments analysed by the third week of treatment. The spatiotemporal data on BMC, BV and TMD revealed that effect of PTH on BMC was mainly due to the changes in bone geometry and bone TMD was not affected by PTH treatment. To our knowledge, this is the first detailed spatiotemporal description of the effect of PTH on the whole mouse tibia. Detecting this level of details was made possible by improving our methodology in two main areas. Firstly, the longitudinal design made possible by the *in-vivo*

μCT imaging, combined with image registration, enabled us to follow each animal over time, and improved the precision of our measurements [17]. Secondly, in the spatial partitioning method, the size of the compartment was optimised to maximise the reproducibility of the measurements, while retaining an excellent description of the changes across the tibia anatomical space [31]. Our previous reproducibility study [31] showed measurements over 40 compartments of mouse tibia (10 longitudinal sections) have a good reproducibility, which implies performing measurements on single slices (and normalised for length) would provide large errors due to the potential differences between an assumed affine growth and a real one. These methodological improvements contributed to a substantial reduction of the variance and a detailed mapping of spatiotemporal bone changes, making it possible to detect smaller and earlier effects, compared to standard 3D bone morphometric analysis. In addition, our partitioning method allows researcher to make comparisons even in young mice, where the changes in length and diameter in long bones due to growth are significant, as our compartments scale with bone growth [31]. The spatially uneven response of bone to PTH raises interesting hypotheses. PTH is a known vasorelaxant and its ostoanabolic activities have been linked to this property [38]. Moreover, the location of Nestin+ mesenchymal stem cells, progenitors of osteoblasts, is around arterioles in areas of higher oxygen concentration [39], which are associated with increased osteoblast function and arteriolar vascularization has been detected in the metaphysis [40]. The observed anabolic effect may therefore be positively associated with higher arterial vascularization. Alternatively, PTH may be increasing bone formation in areas with high biomechanical stimuli. Indeed, there is a growing interest in providing mechanistic insights into the primary and combined effects of PTH and biomechanical stimuli on bone [41, 42]. However, because simple loading conditions were applied in the present study, the correlation between mechanical stimuli and bone changes may not be able to properly highlight the mechanoregulation mechanism.

12

Further investigations, including estimations of physiological loading which the mouse is subjected to during daily activities, controlled *in vivo* mechanical loading [43], and analyses of micro-damage *in vivo*, are required to understand what is the main mechanism (e.g. micro-damage or high strain energy density) associated to the efficacy of the PTH. A detailed mechanistic understanding of the primary effect of PTH on bone may lead to improved protocols of administration alone or in combination with mechanical stimulation.

The FE analysis revealed an increase in the bone stiffness with time for both intervention and control groups. The increase in bone stiffness in the intervention group was significant only after three weeks of treatment, following similar trends as shown by the total BMC. The difference is probably related to the anabolic effect of PTH in most regions after week 21, while the significant increase in the BMC of the most proximal compartments after one or two weeks of treatment was not sufficient to improve the bone mechanical response, at least in the simulated axial compression. The regression analysis showed that the FE predicted stiffness was highly linearly correlated with tibial total BMC. This could be due to the high contribution of cortical thickness (and therefore BMC) in the midshaft in resisting the simulated loading condition. However, it should be noted that the prediction of bone mechanical behaviour from bone total BMC is not trivial and depends on the complex bone geometry, microarchitecture, density distribution and loading scenario. The mechanistic modeling of bone deformation from FE models provides a more comprehensive understanding on how bone deforms under loading and an appropriate estimation of tibial stiffness.

There are some limitations related to this study. First, every invasive measurement inevitably interferes with the experiment; in particular for ionising radiations, the current thinking is that there will always be a non-null probability of biological effects, no matter how small the dose, although the probability decrease linearly as the dose decreases [44].

Therefore, the discussion should be focused on how big such effects are, and how much they affect our conclusions. The comparison with the contralateral, non-irradiated tibia confirmed that the repeated irradiation increased the BMC content by 5% on average, and produced similar effect for both PTH-treated and vehicle-treated mice. What this experiment cannot ensure is that the spatiotemporal patterns we observed in term of PTH effect are not altered by the irradiation. This can be confirmed only if we find similar patterns also when significantly lower radiation dose is used; to the purpose, we are currently developing novel scanning protocols that reduce the radiation dose while preserving the precision of the measurements. Second, the protocol we used to cope with the residual skeletal growth makes possible to monitor the changes in BMC only as average value within a set of 40 relatively coarse compartments, much coarser than what the theoretical spatial resolution of the images would allow. In theory more sophisticated registration techniques such as full elastic registration [45] could provide a mapping of BMC changes with a 10 microns resolution; however, we first need to demonstrate that the errors produced by the registration and the associated image interpolation do not induce precision errors much larger than those obtained with the current method. Third, linear specimen-specific FE models based on a Cartesian mesh have been used to predict the effect of the PTH on the bone stiffness. While we have recently shown for the first time that this μFE approach applied to bovine and human trabecular bone can predict well the distribution of local displacements compared to digital volume correlation measurements [34], the FE models could be further refined and improved by using a smooth tetrahedral mesh, and by implementing material heterogeneities and nonlinearities. Fourth, in this study, the PTH treatment was performed on healthy mature mice while it may be relevant to test a similar approach on old or ovariectomised mice. However, the main goal of this study was to demonstrate the potential of the spatiotemporal analysis and in the future we will test the approach on different animal models. Last, in this

study we have focused on the effect of PTH on the BMC, TMD and BV changes over time because these parameters are simple and highly reproducible [31]. However, this method can be extended to measure other important parameters (e.g. cross-sectional area, moment of area, cortical thickness) in the different sub-regions [10].

In conclusion, we showed that comprehensive analyses of the whole bone provide detailed spatiotemporal characterization of changes in the morphological, densitometric and mechanical properties of the mouse tibia following PTH treatment. The same approach can be used to generate new hypotheses on mechanisms of action of current and future interventions, which would help to design more effective protocols of administration.

Ferrari's group. Researchers are welcomed to contact the corresponding author who will

share the data used in this study.

References

[1] Johnell O, Kanis J. Epidemiology of osteoporotic fractures. Osteoporosis International. 2005;16 Suppl 2:S3-7.

[2] Kanis JA, Johnell O. Requirements for DXA for the management of osteoporosis in Europe. Osteoporosis International. 2005;16:229-38. Epub 2004 Dec 24.

[3] Neer RM, Arnaud CD, Zanchetta JR, Prince R, Gaich GA, Reginster JY, et al. Effect of parathyroid hormone (1-34) on fractures and bone mineral density in postmenopausal women with osteoporosis. N Engl J Med. 2001;344:1434-41.

[4] Li W, Chen W, Lin Y. The Efficacy of Parathyroid Hormone Analogues in Combination With Bisphosphonates for the Treatment of Osteoporosis: A Meta-Analysis of Randomized Controlled Trials. Medicine. 2015;94:e1156.

[5] Bouxsein ML, Pierroz DD, Glatt V, Goddard DS, Cavat F, Rizzoli R, et al. beta-Arrestin2 regulates the differential response of cortical and trabecular bone to intermittent PTH in female mice. J Bone Miner Res. 2005;20:635-43.

[6] Ferrari SL, Pierroz DD, Glatt V, Goddard DS, Bianchi EN, Lin FT, et al. Bone response to intermittent parathyroid hormone is altered in mice null for {beta}-Arrestin2. Endocrinology. 2005;146:1854-62.

[7] Pierroz DD, Bonnet N, Baldock PA, Ominsky MS, Stolina M, Kostenuik PJ, et al. Are osteoclasts needed for the bone anabolic response to parathyroid hormone? A study of intermittent parathyroid hormone with denosumab or alendronate in knock-in mice expressing humanized RANKL. J Biol Chem. 2010;285:28164-73.

[8] Wu X, Pang L, Lei W, Lu W, Li J, Li Z, et al. Inhibition of Sca-1-positive skeletal stem cell recruitment by alendronate blunts the anabolic effects of parathyroid hormone on bone remodeling. Cell stem cell. 2010;7:571-80.

[9] Altman AR, Tseng WJ, de Bakker CM, Huh BK, Chandra A, Qin L, et al. A closer look at the immediate trabecula response to combined parathyroid hormone and alendronate treatment. Bone. 2014;61:149-57.

[10] Bouxsein ML, Boyd SK, Christiansen BA, Guldberg RE, Jepsen KJ, Muller R. Guidelines for assessment of bone microstructure in rodents using micro-computed tomography. Journal of Bone and Mineral Research. 2010;25:1468-86.

[11] de Bakker CM, Altman AR, Tseng WJ, Tribble MB, Li C, Chandra A, et al. muCT-based, in vivo dynamic bone histomorphometry allows 3D evaluation of the early responses of bone resorption and formation to PTH and alendronate combination therapy. Bone. 2015;73:198-207.

[12] Bartlow CM, Oest ME, Mann KA, Zimmerman ND, Butt BB, Damron TA. PTH(1-34) and zoledronic acid have differing longitudinal effects on juvenile mouse femur strength and morphology. J Orthop Res. 2016.

[13] Vrahnas C, Pearson TA, Brunt AR, Forwood MR, Bambery KR, Tobin MJ, et al. Anabolic action of parathyroid hormone (PTH) does not compromise bone matrix mineral composition or maturation. Bone. 2016;93:146-54.

[14] Johnston S, Andrews S, Shen V, Cosman F, Lindsay R, Dempster DW, et al. The effects of combination of alendronate and human parathyroid hormone(1-34) on bone strength are

synergistic in the lumbar vertebra and additive in the femur of C57BL/6J mice. Endocrinology. 2007;148:4466-74.

[15] Wallace RJ, Pankaj P, Simpson AH. Major source of error when calculating bone mechanical properties. J Bone Miner Res. 2014;29:2697.

[16] Dall'Ara E, Boudiffa M, Taylor C, Schug D, Fiegle E, Kennerley AJ, et al. Longitudinal imaging of the ageing mouse. Mechanisms of ageing and development. 2016.

[17] Campbell GM, Tiwari S, Grundmann F, Purcz N, Schem C, Gluer CC. Three-dimensional image registration improves the long-term precision of in vivo micro-computed tomographic measurements in anabolic and catabolic mouse models. Calcified Tissue International. 2014;94:282-92.

[18] Lambers FM, Kuhn G, Schulte FA, Koch K, Muller R. Longitudinal assessment of in vivo bone dynamics in a mouse tail model of postmenopausal osteoporosis. Calcified Tissue International. 2012;90:108-19.

[19] Levchuk A, Zwahlen A, Weigt C, Lambers FM, Badilatti SD, Schulte FA, et al. The Clinical Biomechanics Award 2012 - presented by the European Society of Biomechanics: large scale simulations of trabecular bone adaptation to loading and treatment. Clinical Biomechanics (Bristol, Avon). 2014;29:355-62.

[20] Schulte FA, Lambers FM, Kuhn G, Muller R. In vivo micro-computed tomography allows direct three-dimensional quantification of both bone formation and bone resorption parameters using time-lapsed imaging. Bone. 2011;48:433-42.

[21] Ausk BJ, Huber P, Srinivasan S, Bain SD, Kwon RY, McNamara EA, et al. Metaphyseal and diaphyseal bone loss in the tibia following transient muscle paralysis are spatiotemporally distinct resorption events. Bone. 2013;57:413-22.

[22] Buie HR, Moore CP, Boyd SK. Postpubertal architectural developmental patterns differ between the L3 vertebra and proximal tibia in three inbred strains of mice. J Bone Miner Res. 2008;23:2048-59.

[23] Stadelmann VA, Bonnet N, Pioletti DP. Combined effects of zoledronate and mechanical stimulation on bone adaptation in an axially loaded mouse tibia. Clinical Biomechanics (Bristol, Avon). 2011;26:101-5.

[24] Birkhold AI, Razi H, Weinkamer R, Duda GN, Checa S, Willie BM. Monitoring in vivo (re)modeling: a computational approach using 4D microCT data to quantify bone surface movements. Bone. 2015;75:210-21.

[25] Birkhold AI, Razi H, Duda GN, Weinkamer R, Checa S, Willie BM. The influence of age on adaptive bone formation and bone resorption. Biomaterials. 2014;35:9290-301.

[26] Pereira AF, Javaheri B, Pitsillides AA, Shefelbine SJ. Predicting cortical bone adaptation to axial loading in the mouse tibia. Journal of the Royal Society, Interface / the Royal Society. 2015;12:0590.

[27] Razi H, Birkhold AI, Zaslansky P, Weinkamer R, Duda GN, Willie BM, et al. Skeletal maturity leads to a reduction in the strain magnitudes induced within the bone: a murine tibia study. Acta Biomater. 2015;13:301-10.

[28] Razi H, Birkhold AI, Weinkamer R, Duda GN, Willie BM, Checa S. Aging Leads to a Dysregulation in Mechanically Driven Bone Formation and Resorption. J Bone Miner Res. 2015;30:1864-73.

[29] Casanova M, Herelle J, Thomas M, Softley R, Schindeler A, Little D, et al. Effect of combined treatment with zoledronic acid and parathyroid hormone on mouse bone callus structure and composition. Bone. 2016;92:70-8.

[30] Laperre K, Depypere M, van Gastel N, Torrekens S, Moermans K, Bogaerts R, et al. Development of micro-CT protocols for in vivo follow-up of mouse bone architecture without major radiation side effects. Bone. 2011;49:613-22.

[31] Lu Y, Boudiffa M, Dall'Ara E, Bellantuono I, Viceconti M. Development of a protocol to quantify local bone adaptation over space and time: Quantification of reproducibility. J Biomech. 2016;49:2095-9.

[32] Lu Y, Boudiffa M, Dall'Ara E, Bellantuono I, Viceconti M. Evaluation of in-vivo measurement errors associated with micro-computed tomography scans by means of the bone surface distance approach. Med Eng Phys. 2015;37:1091-7.

[33] Klinck J, Boyd SK. The magnitude and rate of bone loss in ovariectomized mice differs among inbred strains as determined by longitudinal in vivo micro-computed tomography. Calcified Tissue International. 2008;83:70-9.

[34] Chen Y, Dall'Ara E, Manda K, Sales E, Wallace R, Pankaj P, et al. Micro-CT based finite element models of cancellous bone predict accurately displacement once the boundary condition is well replicated: a validation study. Journal of the Mechanical Behavior of Biomedical Materials. 2017; 65: 644-651.

[35] Vickerton P, Jarvis JC, Gallagher JA, Akhtar R, Sutherland H, Jeffery N. Morphological and histological adaptation of muscle and bone to loading induced by repetitive activation of muscle. Proceedings Biological sciences / The Royal Society. 2014;281:20140786.

[36] Webster DJ, Morley PL, van Lenthe GH, Muller R. A novel in vivo mouse model for mechanically stimulated bone adaptation--a combined experimental and computational validation study. Comput Methods Biomech Biomed Engin. 2008;11:435-41.

[37] Bayraktar HH, Keaveny TM. Mechanisms of uniformity of yield strains for trabecular bone. Journal of Biomechanics. 2004;37:1671-8.

[38] Marenzana M, Arnett TR. The Key Role of the Blood Supply to Bone. Bone Res. 2013;1:203-15.

[39] Spencer JA, Ferraro F, Roussakis E, Klein A, Wu J, Runnels JM, et al. Direct measurement of local oxygen concentration in the bone marrow of live animals. Nature. 2014;508:269-73.

[40] Kusumbe AP, Ramasamy SK, Adams RH. Coupling of angiogenesis and osteogenesis by a specific vessel subtype in bone. Nature. 2014;507:323-8.

[41] Gardinier JD, Mohamed F, Kohn DH. PTH Signaling During Exercise Contributes to Bone Adaptation. J Bone Miner Res. 2015;30:1053-63.

[42] Sugiyama T, Saxon LK, Zaman G, Moustafa A, Sunters A, Price JS, et al. Mechanical loading enhances the anabolic effects of intermittent parathyroid hormone (1-34) on trabecular and cortical bone in mice. Bone. 2008;43:238-48.

[43] Birkhold AI, Razi H, Duda GN, Weinkamer R, Checa S, Willie BM. Mineralizing surface is the main target of mechanical stimulation independent of age: 3D dynamic in vivo morphometry. Bone. 2014;66:15-25.

[44] Preston RJ. Update on linear non-threshold dose-response model and implications for diagnostic radiology procedures. Health Physics. 2008;95:541-6.

[45] Dall'Ara E, Barber D, Viceconti M. About the inevitable compromise between spatial resolution and accuracy of strain measurement for bone tissue: a 3D zero-strain study. J Biomech. 2014;47:2956-63.
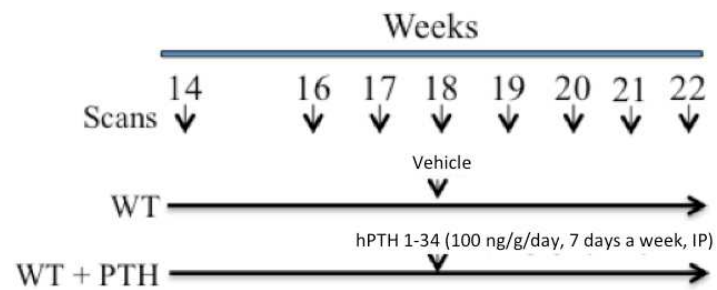
Figure 1: Overview of the experimental design. Scans were performed at week 14 and then weekly from week 16 to week 22. Starting from week 18, mice received a daily i.p. injection of PTH ("WT+PTH" group, 100ng/g/day) or vehicle ("WT" group) 7 days a week.
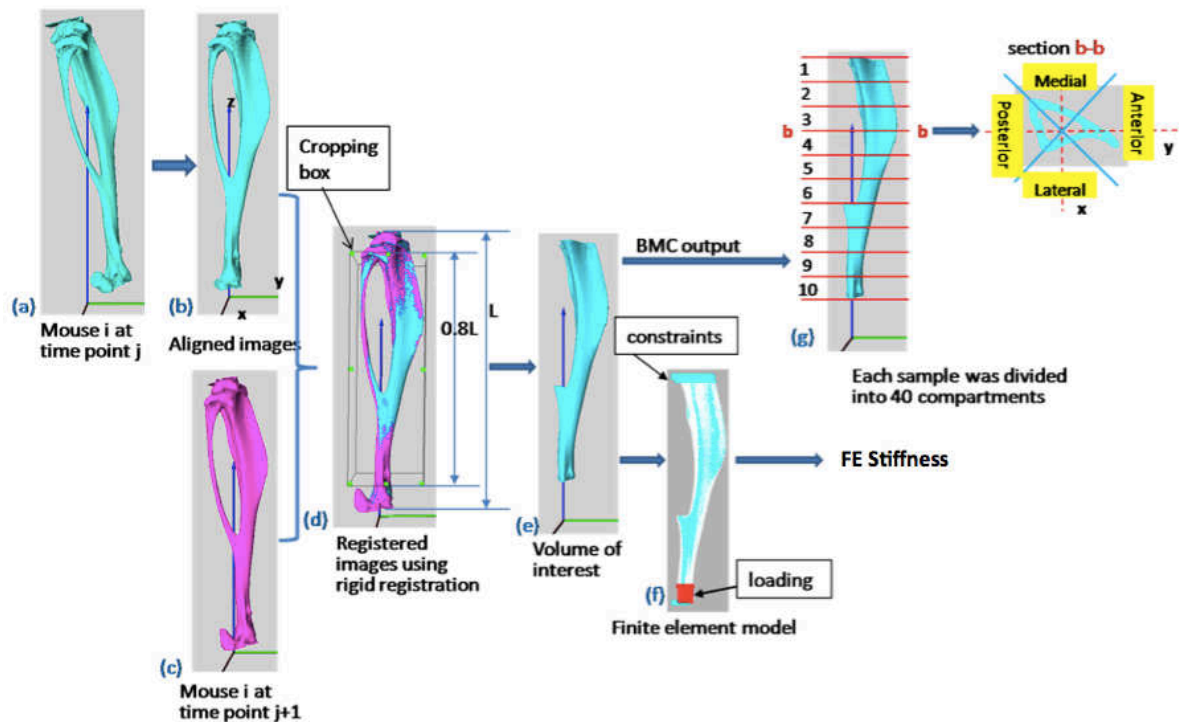
Figure 2: Schematic representation of the partitioning of the tibia into 40 compartments. The tibia from the baseline scan serves as reference (a) and the tibiae from the following scans(c) and from other mice are rigidly registered to it (d). After the image transformation, the tibial length (L) is measured and a region of 80% of L is cropped out starting from the area below the proximal growth plate. The tibia volume of interest (VOI)(e) was converted into subject-specific finite element (FE) models (f) for the estimation of compressive. The bone mineral content was computed in 40 regions, after dividing the VOI into ten sections with the same length along the tibia longitudinal (proximal-distal) direction and dividing each section into four sectors (anterior, medial, posterior and lateral sectors) according to the centre of mass of each slice (g).

Lateral

	16	17	18	19	20	21	22
C01	0	1	-5	6	5	10*	13**
C02	0	1	-3	4	5	10**	12**
C03	0	3	0	4	7	13**	13**
C04	0	3	-2	3	6	12**	13**
C05	1	2	-2	2	6	13**	15**
C06	1	1	-4	2	4	11*	12**
C07	0	4	-1	3	2	8	10
C08	1	3	-1	4	5	10*	11**
C09	-5	-2	-8	1	2	10*	11**
C10	-5	-1	-8	-3	-1	4	6

Medial

	16	17	18	19	20	21	22
C01	0	1	-2	9*	9*	15**	15**
C02	5	4	3	10	10	18**	18*
C03	1	-1	-2	6	8	19**	16**
C04	-1	-2	-2	4	11*	16**	17**
C05	0	0	0	4	9*	17**	18**
C06	-1	0	-2	3	6	12**	13**
C07	1	2	-1	4	3	10**	12**
C08	0	1	-2	1	-1	7	10**
C09	-1	0	-1	4	2	8	7*
C10	-2	1	-5	1	1	7	10**

Anterior

	16	17	18	19	20	21	22
C01	2	3	-1	5	11**	14**	20**
C02	1	1	-2	3	8*	11**	17**
C03	0	1	-1	5	7	8*	11**
C04	1	1	-2	4	6	10**	11**
C05	1	1	0	4	4	11**	12**
C06	0	0	-1	3	5	10**	12**
C07	-1	0	-1	4	6	11**	14**
C08	2	1	2	4	4	9**	12**
C09	-1	-1	1	0	0	6	9**
C10	-3	-2	-2	2	7	9*	12**

Posterior

	16	17	18	19	20	21	22
C01	1	3	-1	7*	9*	16**	19**
C02	-1	2	-1	5	10**	12**	15**
C03	0	2	-1	6	7	12**	13**
C04	-1	0	-4	3	4	9*	11**
C05	2	3	-3	4	5	11*	12**
C06	1	2	-3	4	5	10*	11**
C07	-3	-2	-5	3	5	10*	12**
C08	2	2	1	4	1	8*	10**
C09	3	4	2	6	1	9*	10**
C10	0	2	-1	7	3	14**	14**

-20　-10　-3　0　3　10　20

▬ Intermittent PTH treatment (from 18 weeks of age until the end of the experiment)

*Figure 3: The spatiotemporal effect of PTH on tibial regional bone mineral content (BMC). Data are expressed as the weekly mean relative percentage difference of changes in BMC between the PTH and the control group for the 10 sub-divisions along the tibial axis, for each of the 4 anatomical positions (Lateral, Medial, Anterior and Posterior). Table colour code: The grey areas are values within our measurement error range, therefore with no significant changes. The red areas represent an anabolic effect. * p<0.05, ** p<0.01 vs WT. N= 5 mice.*

Lateral

	16	17	18	19	20	21	22
C01	-1	-1	-3	1	1	2	2
C02	-1	0	-3	1	1	2	1
C03	-2	0	-2	1	2	1	1
C04	-1	1	-1	1	2	0	1
C05	0	0	-1	0	1	0	1
C06	0	0	-1	1	1	1	0
C07	0	0	-1	1	0	1	0
C08	0	0	-1	1	0	1	1
C09	-1	0	-1	0	1	0	1
C10	0	1	0	1	0	1	0

Medial

	16	17	18	19	20	21	22
C01	0	1	-2	4	3	4	2
C02	-1	2	2	3	2	3	1
C03	-1	-1	-5	-1	0	4	1
C04	-1	-2	-2	-1	2	1	1
C05	0	-1	-1	0	1	1	0
C06	-1	-1	-1	0	1	1	0
C07	0	0	-1	1	1	2	1
C08	-1	-1	-2	0	1	1	1
C09	0	0	0	2	2	1	1
C10	1	1	0	3	1	2	1

Anterior

	16	17	18	19	20	21	22
C01	-1	0	-2	1	2	0	0
C02	0	0	-1	0	0	2	1
C03	0	0	-1	1	1	1	0
C04	0	0	-2	1	1	1	0
C05	-1	0	-2	2	1	1	1
C06	-1	0	-1	1	2	0	1
C07	0	0	0	1	1	0	0
C08	-1	-1	-2	0	1	0	0
C09	-1	-1	0	-1	0	-1	0
C10	0	-1	0	0	1	0	0

Posterior

	16	17	18	19	20	21	22
C01	-1	0	-2	2	3	2	2
C02	0	1	-2	1	2	0	1
C03	-1	1	0	2	3	0	2
C04	-1	0	-1	1	2	0	1
C05	-1	1	-2	1	1	0	1
C06	-1	1	-1	2	1	0	0
C07	0	1	-1	1	1	1	0
C08	-1	0	-2	0	1	0	0
C09	0	1	0	2	1	1	1
C10	0	1	-1	3	0	2	1

-20   -2   2   20

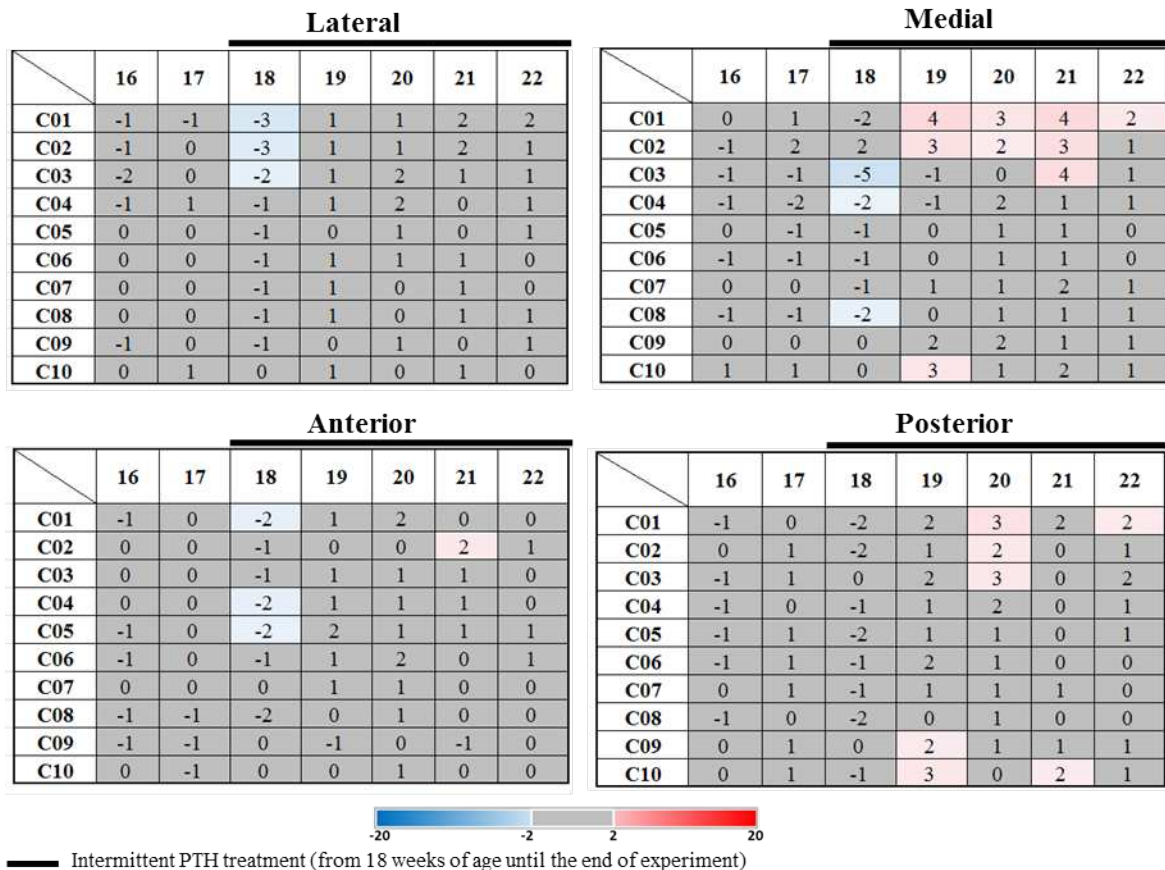━━ Intermittent PTH treatment (from 18 weeks of age until the end of experiment)

Figure 4: The spatiotemporal effect of PTH on tibial regional bone tissue mineral volume (TMD). Data are expressed as the weekly mean relative percentage difference of changes in TMD between the PTH and the control group for the 40 compartments. Table colour code: The grey areas are values within our measurement error range, therefore with no significant changes.
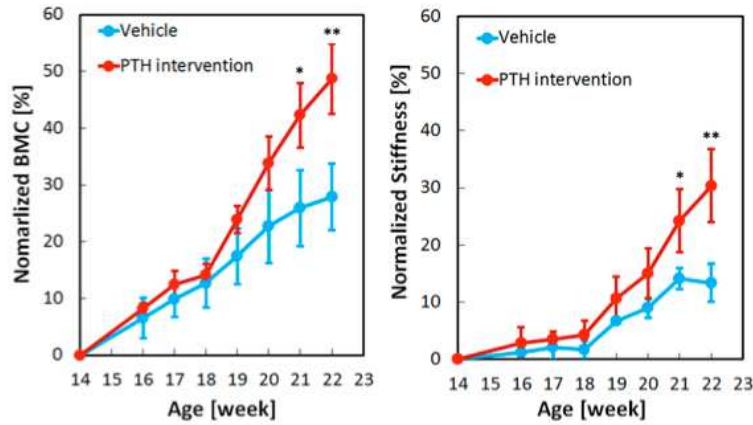
Figure 5: Longitudinal effect of PTH intervention on total tibial BMC and FE predicted stiffness over the temporal scale. Data presented as mean standard deviations of the normalized data with respect to baseline (*p<0.05,**p<0.01).
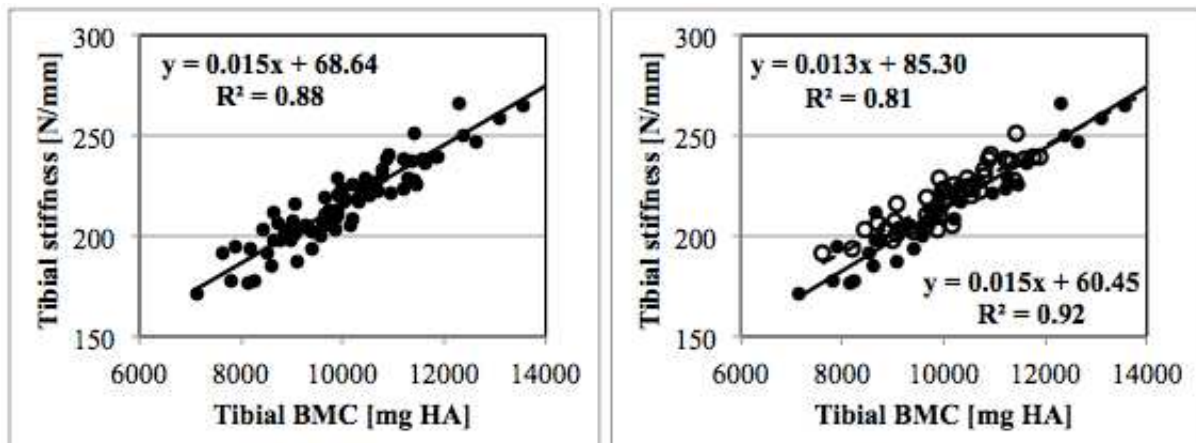

Figure 6: Linear regression analysis for predicted stiffness vs BMC for data pooled for both PTH intervention and vehicle groups (left) or separated (right; PTH intervention in full circles and bottom right equations; vehicle group in open circles and top left equations).